Giraldo Jorge A. (Orcid ID: 0000-0003-4906-5406)
Sierra Carlos A. (Orcid ID: 0000-0003-0009-4169)

Tree growth periodicity in the ever-wet tropical forest of the Americas

Jorge A. Giraldo[1] ORCID: 0000-0003-4906-5406

Jorge I. del Valle[1] ORCID: 0000-0001-5908-7575

Sebastián González-Caro[1]

Diego A. David[1]

Tyeen Taylor[2] ORCID: 0000-0002-0926-098X

Conrado Tobón[1] ORCID: 0000-0001-8372-0625

Carlos A. Sierra[3,4] ORCID: 0000-0003-0009-4169

[1] Departamento de Ciencias Forestales, Universidad Nacional de Colombia, Medellín, Colombia

[2] Department of Civil & Environmental Engineering, University of Michigan

[3] Max Planck Institute for Biogeochemistry, Jena, Germany

[4] Swedish University of Agricultural Sciences, Uppsala, Sweden

Key words: Tree rings, rainiest place on Earth, *Chocó* Biogeographic Region, dendrometers.

Running head: Tree rings in the ever-wet tropical forest

Corresponding author: Jorge A. Giraldo, jagiral1@unal.edu.co

Abstract

1. The occurrence of annual growth rings in tropical trees—the result of the seasonal activity of vascular cambium—has been explained by seasonal water deficit or flooding periods. However, little is known about the drivers of annual tree-ring formation under tropical hyper-humid conditions without clear seasonal dry periods or flooding (ever-wet conditions). Shelford's law states that the deficit or the excess of environmental resources limit plant growth. Accordingly, we hypothesize that excess soil moisture, a slight seasonal reduction of precipitation, and a reduction in light availability, determine rhythmic growth in ever-wet tropical forests.
2. We first assessed the occurrence of rhythmic growth in 14 tree species from the Biogeographic Chocó Region (annual rainfall 7,200 mm) using three methods: Radiocarbon (^{14}C) dating (all studied species), tree ring synchronization (4 species that have replicates), and automatic dendrometers (two species). Then, we assessed the effect of environmental drivers (rainfall, short wave radiation, temperature, and soil moisture) on tree growth based on tree ring and dendrometer observations.
3. We present evidence of annual tree-ring formation in all 14 studied tree species. Depending on the tree species, we observed positive and negative correlations between growth, water availability, and light availability. These relationships suggest that both excess or deficit of environmental resources may explain the seasonal pattern of tree growth. Although we cannot differentiate between excess soil water and low light availability by high cloudiness, we suggest that cloudiness frequency could affect tree growth in these forests.
4. *Synthesis*. We reveal the annual formation of growth rings in the unexplored wetter-end tropical forests, where seasonal growth depends on either high soil moisture and hypoxia or light limitations by cloudiness and photosynthesis constraints.

Introduction

Carbon storage and sequestration in natural vegetation mitigates the climate effect of anthropogenic CO_2 emissions (Pan et al., 2011). Carbon fluxes are large in tropical forests such as Amazon forests, however the magnitude of these fluxes change across space according to climatic conditions (e.g., temperature and rainfall seasonality) and biotic processes (e.g., species composition) that ultimately control plant CO_2 fixation (i.e., plant productivity) (Muller-Landau et al., 2021) and respiration. For example, plant productivity is lower in tropical dry forests relative to humid forest, suggesting rainfall amount as a regional driver of plant productivity gradients across the tropics (Muller-Landau et al., 2021), but little is known about plant productivity under higher rainfall amounts (Posada & Schuur, 2011; Schuur, 2003). Therefore, understanding the drivers of tropical plant productivity at the wetter end of the precipitation gradient is essential for determining globally relevant carbon dynamics.

In forests, plant productivity is usually studied on permanent sampling plots, both at the community and at individual plant levels (i.e., plant growth) (Babst et al., 2014; Zuidema et al., 2013). On regional to global scales, carbon sinks are identified employing a combination of remote sensing data and micro-meteorological measurements combined with ecosystem C models (Araza et al., 2022; Avitabile et al., 2016; Beer et al., 2010; N. G. McDowell et al., 2015). Individual tree growth data are often necessary to calibrate broad-scale estimations and understand ecological drivers of plant productivity (Albert et al., 2019; Muller-Landau et al., 2021; Zuidema et al., 2022; Zuidema & Van der Sleen, 2022). In the tropics, one of the most important drivers of plant growth is water availability (Esquivel-Muelbert et al., 2017; Wagner, Rossi, Stahl, Bonal, & Hérault, 2012). Many studies have shown that individual plant growth is reduced under low water availability or droughts, affecting carbon uptake and increase hydraulic

failure (Corlett, 2016; N. McDowell et al., 2018). Likewise, plant growth is also limited by high water availability such as flooding (i.e., water excess), in which soils are saturated and reduce their metabolism (Costa, Schietti, Stark, & Smith, 2022; Esteban, Castilho, Melgaço, & Costa, 2021). Therefore, both water availability extremes can limit tree growth (Schuur, 2003). Extremes of each condition or resources are indeed expected to limit species performance according to Shelford's law (Costa et al., 2022; Giraldo, del Valle, Sierra, & Melo, 2020; Shelford, 1931).

Ecological studies mainly focused on the lower limit of water availability gradient because drought is the main concern under current and future climate change scenarios (Corlett, 2016; Hammond et al., 2019; Konings et al., 2021). Similarly, understanding how plants respond to water excess is limited to flooded forests, but there is a paucity of studies in humid forests receiving high rainfall throughout the year ($\geq$ 2000 mm y^{-1}) and lacking a dry season (year-round precipitation > 100 mm $month^{-1}$, hereafter "ever-wet forests") (Underwood, Olson, Hollander, & Quinn, 2014). Considering that climate models predict that precipitation and water availability will increase in the future, wet regions will get wetter by at least 10% in the wettest tropical forests (Schurer, Ballinger, Friedman, & Hegerl, 2020). Knowing the response of plant growth under the wet extreme will give a more nuanced understanding of the responses of tropical forests as a whole.

Tree growth rhythms are seasonal events occurring in tissues or organs such as meristems, roots, leaves, and reproductive structures (Albert et al., 2019; Lüttge & Hertel, 2009) that are driven by seasonal climate conditions and soil nutrients (Fyllas et al., 2017). In particular, the seasonality of vascular cambium development produces visually distinct rings in tree wood, which are helpful

for measuring tree growth. In temperate regions, periodic growth ring formation is commonly driven by strong annual variability in temperature and day length (e.g., the annual seasons) (Babst et al., 2018; Pearl et al., 2020; Stine, 2019). In contrast, the stability of day length and temperature in the tropics highlights the role of water availability (i.e., precipitation seasonality or flooding) as the main driver of tropical tree-ring formation (Rozendaal & Zuidema, 2011). Scientific evidence of tropical annual tree rings mainly comes from tree species from both seasonally dry and seasonally flooded forests (Giraldo et al., 2020), demonstrating that both water deficit and excess determine seasonal growth patterns (Brienen, Schöngart, & Zuidema, 2016; Rozendaal & Zuidema, 2011; J. Schöngart, Bräuning, Barbosa, Lisi, & Oliveira, 2017). However, the periodicity of tree-ring formation in ever-wet tropical forests and its potential drivers remain understudied (Giraldo, del Valle, González-Caro, & Sierra, 2022; Giraldo et al., 2020).

There is already evidence of tree-ring formation in ever-wet tropical forests. Giraldo et al. (2020) showed a high percentage of tree species with tree-ring structures (66 out of 81 tree species) from the *Chocó* region in northwestern South America, the rainiest region in the Americas with no evidence of seasonality in ecosystem productivity (Estupinan-Suarez et al., 2021). While it is not clear what factors control periodic growth rhythms in tropical trees under such conditions, slight variation in rainfall, soil moisture, solar irradiance, cloudiness, and sunrise - sunset times are hypothesized as potential environmental drivers (Borchert & Rivera, 2001; Breitsprecher & Bethel, 1990; Clark & Clark, 1994; Giraldo et al., 2022, 2020). Light availability, namely photosynthetically active radiation (PAR), is a limiting factor in high cloud-cover regions such as ever-wet tropical forests (Restrepo-Coupe et al., 2013). In the wettest forests, we can expect extreme light limitation during the rainiest months, which would likely produce an annual pattern

in tree growth. Indeed, tree growth in tropical forests with distinct precipitation seasonality is limited by light availability during the rainy season (Graham, Mulkey, Kitajima, Phillips, & Wright, 2003). This implies either reduction in growth and productivity during the rainiest months because of soil water excess (Costa et al., 2022), or photosynthetic limitation caused by high cloudiness and precipitation (Restrepo-Coupe et al., 2013). Therefore, in ever-wet forests that lack a dry season, water availability may be close to the maximum tolerance threshold for some species. High soil water saturation favors root hypoxia limiting tree growth (Esteban et al., 2021; Sauter, 2013). Based on these facts, we expect to find negative correlations between the rainiest months and tree growth in the wettest tropical forests.

Here, we combined different approaches to estimate tree-ring periodicity, such as radiocarbon dating (^{14}C measured in tree rings), crossdating (tree-ring synchronization among individuals of the same species), and dendrometer observations (automated high-resolution stem increment measurements) on 14 tree species from an ever-wet tropical forest in the *Chocó* region of Colombia. We hypothesized that light, soil moisture, and slight reductions in precipitation control tree growth rhythm in ever-wet tropical forests that lack evident dry periods. Therefore, we aim, to i) determine the frequency of tree-ring formation in trees, and ii) assess the environmental drivers of tree growth in an ever-wet tropical forest. We expect this information to provide new insights on the interaction between physiology and environmental drivers of growth rhythms in ever-wet tropical forests.

Materials and methods

Study area

We carried out this study at the lower *Calima* River basin (LCRB) (3°57′12.54′′ N, 76°59′27.96′′ W), within the *Chocó* Biogeographic Region in northwestern South America, near Colombia's Pacific coast (Figure 1), which is the rainiest region in the Americas. In some places, the mean annual rainfall is higher than 12,000 mm (Mesa & Rojo, 2020; Poveda & Mesa, 2000). In 2018, 26,987 mm of rainfall was recorded in the *Yurumanguí* village, 120 km south of our study area (Mesa & Rojo, 2020). The high regional precipitation is associated with the low-level jet stream (tropopause air current) centered around 5°N, known as the *Chocó* Jet (Mesa & Rojo, 2020). Furthermore, the high floristic richness and endemism make the *Chocó* region one of the most biodiverse hotspots on Earth (Myers, Mittermeler, Mittermeler, Da Fonseca, & Kent, 2000; Pérez-Escobar et al., 2019). Small hills with slopes up to 45° and elevations 40 - 100 m asl characterize the topography of the study area. Soils are mottled gray-yellow clay-loam, poor in soil nutrients, with high iron and aluminum concentrations (Faber-Langendoen & Gentry, 1991).

Tree-ring sampling and frequency determination

We obtained stem cross-sections of tree species sampled opportunistically. We accompanied local Afro-Colombian ethnic groups that sporadically harvest trees for economic and cultural activities. Among the collections, we selected 14 species (Figure 2) with both clearly distinct and indistinct tree rings (Giraldo et al., 2020) to establish their frequency by the radiocarbon bomb-peak method (del Valle & Giraldo, 2021; del Valle, Guarín, & Sierra, 2014; Worbes & Junk, 1989). A priori, we assumed tree-ring formation was annual for dendrochronological dating. Then, we assigned the corresponding calendar year to the last ring formed as the sampling year (2016 or 2017). From the last ring (closest to the bark) to the pith, we determine the corresponding calendar year by counting backward. We collected wood samples (approx. 20 mg) from selected rings for radiocarbon analysis. We extracted alpha cellulose following Steinhof et

al., (2017). ^{14}C of sampled wood was determined by the Radiocarbon Laboratory of the Max Planck Institute for Biogeochemistry in Jena, Germany. We calibrated the radiocarbon results using CaliBomb (Reimer, Brown, & Reimer, 2004) and the Northern Hemisphere Zone 2 curve. We smoothed a one-year function to obtain calendar dates from the radiocarbon values.

Intraspecific tree-ring synchronization

To assess tree-ring synchronization, we evaluated multiple individuals ($n \geq 5$ trees) belonging to four species*:* *Humiriastrum procerum* (Hp), *Qualea lineata* (Ql), *Apeiba macropetala* (Am), and *Goupia glabra* (Gg). We selected conspecific trees growing in similar sites and conditions (light exposure and slope). Our study area bears an exceptional richness and diversity of tree species with many endemic and rare species (Gentry, 1989), and accordingly, the population of each species is typically small. Most tree species sampled are distributed sparsely over the landscape, which limits the availability of conspecific replicate trees. Samples were prepared according to standard procedure as described by Speer (2010). High-resolution images of wood cross-sections (1800-2400 dpi) were obtained with an Epson Expression 10000XL scanner (Epson America, Inc), allowing us to observe wood features down to 10-15 µm. We measured growth rings by combining ImageJ (Fiji, V11.52i) (Schindelin et al., 2012) and R software (R Core Team, 2020). We cross-dated at both the individual and species levels. First, we compared multiple radii within the same tree, then we gradually added tree-ring series from other individuals of the same species, ensuring statistical and graphical synchronization. We use the *dplR* package (Bunn, 2008, 2010) for quality control, series synchronization, and generation of chronologies.

Intra-annual dendrometer growth measurements

To measure stem increment changes to a high temporal resolution, we installed an automatic band dendrometer (Tree-Hugger®, Global Change Solutions) on each of 20 trees (height: 25-30 m), with diameters from about 15-30 cm and heights from 1.3 to 3 m above the ground to avoid buttresses. Measurements were recorded hourly and downloaded every five weeks. Before installing the dendrometers, we cleaned the stem surfaces to avoid epiphyte proliferation around the bark. We installed the first ten dendrometers in April 2018. Most of them stopped recording after several months. We installed a second group in October 2019; most were still working until our last download in February 2021. Device problems were attributable to the permanently high relative humidity in the study area. For the dendrometer measurements, we selected two species with clearly distinct tree rings: *G. glabra* ($n = 6$), and *A. macropetala* ($n = 3$). In order to obtain gapless annual dendrometer records, we combine growth-rate-standardized data from replicate trees within each species. They are included in the analysis of our tree-ring series (see above). As a first step, we transformed circumference increment data into radial increment data under the assumption of cylindrical stems. We averaged the monthly stem increment data, thus smoothing the noise caused by short-term fluctuations of stem girth due to daily changes in soil humidity and diurnal fluctuations of temperature and radiation. We obtained the mean monthly, cumulative, and standard deviation of the growth increments for an entire year. We performed all filter procedures and statistical analyses using R (R Core Team, 2020).

Environmental data

Monthly rainfall data (1947- 2017) and monthly temperature data (1957-2016) were available from the *Bajo Calima* meteorological station managed by Colombia's weather service (IDEAM). Due to the lack of ground instrumental measurements of solar radiation, we used a satellite-derived product of mean monthly short-wave solar radiation (SWR, W m^{-2}) available from

Clouds, and the Earth's Radiant Energy System - CERES (https://ceres.larc.nasa.gov/) (Kato et al. 2013), as a surrogate for incoming photosynthetically active radiation (2000-2019). The Normalized Difference Vegetation Index (NDVI, or vegetation 'greenness'), a proxy for photosynthetic capacity) was obtained from the MODIS MOD13Q1 product. The NDVI time series were filtered by removing clouds and low-quality data. We extracted these data from the MODISTools R package (Tuck et al., 2014). We used a 1km x 1km window centered on the study site. We selected pixels where forest cover has been maintained for the last 20 years. For each point, we averaged NDVI data for each month between 2000 and 2019. Finally, we installed two soil moisture (TDR, Time Domain Reflectometry) and soil temperature stations (Campbell Sci®) with sensors installed at two depths: 10 and 30 cm, at sites representative of the study tree environments, logging at 30 min frequency between 2018 and 2020. Sensor representation of soil water content was calibrated according to Frumau et al. (2006).

Data analysis

To determine the frequency of tree-ring formation, we first compared calibrated dates and dendrochronological dates using a linear model. Counting the number of rings between two dated rings allowed us to establish their frequencies (del Valle et al., 2014)). Second, we evaluated tree-ring synchronization within species with standard dendrochronological metrics: The series intercorrelation, which measures the strength of a common signal in all sampled trees, and the mean correlation coefficient among tree-ring series (r), which is an indicator of signal strength similarity (Cook & Pederson, 2011; Speer, 2010). We also used the expressed population signal (EPS) metric, which measures shared variability within a chronology. Values below 0.85 suggest few trees dominate the signal (Speer, 2010). The Signal-to-noise ratio (SNR) measures the amount of the desired signal recorded in a chronology (Cook & Kairiukstis, 1992; Speer, 2010).

Mean sensitivity is a measurement of variability in tree ring widths, values ranging between 0.2 and 0.4 are considered sensitive enough for climate reconstruction (Speer, 2010).

To assess the relationship between the frequency of tree-ring formation and environmental parameters, we used the R-package Treeclim (Zang & Biondi, 2015) to perform bootstrapped correlation analyses between tree-ring chronologies and the following variables: mean monthly precipitation, mean monthly temperature, and SWR (W m^{-2}) in annual sets, from September to August (phenological year). We chose September-August as the phenological year based on our field observations: leaf turnover between September to February and flowering between February-May. We used the NDVI time series as complementary information to support phenological changes in the canopy for the study area. Finally, to assess the effect of environmental drivers on intra-annual tree growth, we used a cross-correlation test between monthly dendrometer series from two species (*G. glabra* and *A. macropetala*) and these variables: monthly data of precipitation, soil water content, short-wave radiation (SWR), and temperature.

Results

Frequency of tree-ring formation

We observed a tight correlation between ^{14}C calibrated tree-ring dates and dendrochronological dates derived by counting rings backward from the sample date and assuming annual frequency (36 samples from 14 species combined, $R^2 = 0.99$, $p < 0.001$, Figure 3 and Table S1). According to this result, in the 14 species tested, tree-ring formation occurs annually (Table S1, Figure S1 and Figure S2). Four species with a single dated ring were also consistent with annual periodicity in tree-ring formation. The absolute difference between all radiocarbon vs. dendrochronological

dates was within a one-year margin (mean = 0.44-year, sd. = ± 0.31-year) (Figure 3). The phenological year usually does not coincide with the calendar year. This mismatch can produce the observed small differences in Figure 3. In just one sample of *Tachigali colombiana* (Tc), we found the highest deviation (1.5 years) between calibrated ^{14}C and dendrochronology dates (Figure 3b). This error is likely due to sampling by taking some wood from an adjacent ring. However, the annual nature of the tree rings of this species is confirmed both in tree rings of the same individual and from other trees of the same species (Figure 3).

Tree-ring synchronization

Four species, *H. procerum*, *Q. lineata*, *A. macropetala*, and *G. glabra,* with a sample size between 5 and 12 trees growing under similar conditions, were successfully cross-dated. Despite the small sample available, we confirmed the synchronization of the tree rings (Table 1). Two species with the highest number of replicates, *Q. lineata,* and *G. glabra*, presented suitable values of serial correlation (0.42 – 0.46, $p < 0.05$, respectively), running *r-bar* (0.36 – 0.31, respectively) and EPS (0.87 – 0.89, respectively) (Table 1). The other two species had the highest and the lowest mean series correlation: *A. macropetala* (0.49, $p < 0.05$) and *H. procerum* (0.41, $p < 0.05$), respectively. Both species also revealed low EPS values (Table 1). *H. procerum* and *G. glabra* are prone to form wedging rings close to wounds, where tree rings usually vanish. We carefully avoided those sectors in cross-sections when delineating and measuring growth rings. Figure 4 represents tree-ring chronologies generated for these species.

Tree-ring series vs. environmental variables

Chronology-climate correlations differed between species (Figure 5). *H. procerum* showed a negative association with September precipitation of the previous year ($r = - 0.33$, $p < 0.05$) and

with mean precipitation from September-October of the concurrent year (r = - 0.35, $p < 0.05$) (Figure 5a). The chronology of this species was also significantly correlated with shortwave radiation from the previous October and concurrent January (October: r = -0.54, $p < 0.05$; January: r = 0.66, $p < 0.05$), and it also correlated with mean short-wave radiation from the previous December to concurrent April (r = 0.56, $p < 0.05$) (Figure 5e).

The growth of *Q. lineata* was significantly and positively associated with January precipitation of the current year (r = 0.38, $p < 0.05$) and with mean precipitation from September (previous year) to January (r = 0.28, $p < 0.05$) (Figure 5b), but negatively correlated with shortwave radiation of the previous December (r = -0.45, $p < 0.05$) (Figure 5f).

The chronology of *A. macropetala* was negatively correlated with June and July precipitation of the concurrent year (June: r = -0.58, $p < 0.05$; July: r = -0.34, $p < 0.05$) (Figure 5c) and with mean precipitation from concurrent May to current September (r = -0.44, $p < 0.05$) (Figure 5c). Also, positively correlated with shortwave radiation of the previous October, previous November, concurrent March and concurrent April (October: r = -0.65, $p < 0.05$; November: r = -0.61, $p <$ 0.05; March: r = 0. 68, $p < 0.05$; April: r = 0.59, $p < 0.05$) (Figure 5g). The chronology of this species was also correlated with the mean concurrent year's shortwave radiation from January to May (r = 0.77, $p < 0.05$) (Figure 5g).

The tree-ring chronology of *G. glabra* was positively associated with May, July and August precipitation of the concurrent year (May: r = 0.23, $p < 0.05$; July: r = 0.40, $p < 0.05$; August: r = 0.31, $p < 0.05$), and positively correlated with mean precipitation from May to October of the concurrent year (r = 0.43, $p < 0.05$) (Figure 5d). Its growth was negatively correlated with

shortwave radiation in March of the concurrent year (r = -0.42, p < 0.05) and with mean shortwave radiation from January-June of the concurrent year (r = -0.36, p < 0.05) (Figure 5h). Temperature had non-significant associations with the analyzed chronologies (Figure S3).

Dendrometer growth vs. environmental variables

Dendrometer measurements provide evidence of similar intra-annual growth rhythms in the two species with a temporal offset of approximately three months (Figure 6 and Figure S4). *A. macropetala* showed a four-month of peak cumulative growth from February to May, while *G. glabra* showed a similar four-month period of peak cumulative growth from May to August (Figure 6a).

Dendrometer measurements provide evidence of intra-annual growth rhythms occurring differently in the two studied species (uncoupled growth) (Figure 6a). *A. macropetala* growth is evident from January to August, followed by a shrinkage (contraction) of the stem from August to October. Growth then increases again from November to December. These results suggest that the growth cycle begins in November of the previous year and ends in August of the current year. Dendrometer data from *G. glabra* revealed no growth and slight shrinkage from January to March, followed by growth from April to October, then an abrupt shrinkage and no growth from October to December. In summary, the two species have similar patterns of growth phenology but with a three-month offset. Thus, the phenological year starts in March and ends in February.

Figure 6a shows variations in tree growth and some environmental factors throughout the year. We assessed by cross-correlation analysis time-lagged correlations between growth and environment (Figure 6b). In both species, cumulative growth positively correlated with

precipitation with no time lag for *G. glabra* and a two-month lag for *A. macropetala* (Figure 6b). The relationship between SMC and both species presents the highest significant correlation value with a lag of 2 months (Figure 6b). A significant negative correlation, with 2 and 3 months lagged, was observed between *G. glabra* and SWR (Figure 4b); no relationship was observed between *A. macropetala* and SWR (Figure 6b).

Discussion

Our results show, for the first time, the prevalence of annual tree rings in ever-wet tropical forests and their potential association with environmental conditions. We present evidence of annual tree-rings in all 14 studied tree species (Figure 3). This is the first report of annual tree rings for *Inga acreana*, *I. rubiginosa*, *Mabea sp*, *Otoba latialata*, *Pterandra ultramontana*, *Qualea lineata*, and *Tachigali colombiana*. This paper adds new species (some endemic to the *Chocó* region) to the 284 tropical tree species previously reported in tree-ring databases (Locosselli et al., 2020). Our findings in the rainiest forest of the Americas challenge the assumption of a lack of seasonal growth and the absence of tree rings in trees from wetter-end environments (De Micco et al., 2019; Schweingruber, Börner, & Schulze, 2008).

We hypothesized that rainfall seasonality influences annual tree rings through a direct negative effect of water excess on tree growth. We found partial support for this hypothesis from our results based on tree-ring synchronization in two species. In *H. procerum* and *A. macropetala*, tree-ring indices were negatively correlated with the rainiest season of the year (Figure 5). In addition, the maximum growth rate of *A. macropetala* occurred during the less rainy season, and growth stopped during the rainiest season (Figure 6). Both species are also deciduous during the rainiest period between July and October (CONIF, 1996). Reduced growth may be driven by soil

saturation, leading to root hypoxia (Dezzeo, Worbes, Ishii, & Herrera, 2003; Esteban et al., 2021), similarly as in Amazon floodplains. Annual seasonal root flooding coincides with leaf deciduousness, reduced growth, and tree ring formation (Jochen Schöngart, Piedade, Ludwigshausen, Horna, & Worbes, 2002). High soil moisture likely limits, during the wettest months, the growth of trees at our site due to root hypoxia. However, our field measurements evidenced little intra-annual variation of soil moisture content, following the annual rainfall pattern (0.59 ± 0.003 cm^3 cm^{-3}) (Figure 6a). This suggests that the high soil moisture and its effect on root hypoxia are unlikely to explain seasonal patterns in tree growth.

Alternatively, reduced light caused by high cloudiness during rainy periods may cause seasonal reductions in tree growth (Restrepo-Coupe et al., 2013; Saleska et al., 2016; Wu et al., 2016). In both species (*H. procerum* and *A. macropetala*), tree-ring indices negatively correlated with the rainiest season of the year. Conversely, they positively correlated with solar radiation during the less rainy months of the year (Figure 5). Based on dendrometer data for *A. macropetala*, the maximum growth rates occur during the less rainy months, and growth stops during September - October, the rainiest months, and is weakly related to solar radiation (Figure 6). These tree species may have developed strategies to maximize their carbon uptake (i.e., photosynthetic activity) during short periods of relatively high solar radiation. Accordingly, we would expect high leaf flushing in the less rainy months (Saleska et al., 2016); or leaf shedding during the rainiest months to avoid low solar radiation levels. In contrast, NDVI increased after the less rainy period (Figure 1e), with higher solar radiation potentially promoting leaf production of the light-limited tree species (Restrepo-Coupe et al., 2013). Further work is required to assess potential mechanisms relating light limitation to the seasonality of growth in ever-wet tropical forests, including phenological observations (e.g., in-situ phenocams), leaf-level CO_2 assimilation

rates, seasonal variability of non-structural carbohydrates and remote sensing estimates of the phenology.

Multiple sources of evidence (ecological, satellite, eddy covariance and phenocam observations) have shown a strong role of solar radiation in non-water limited forest trees (e.g., ever-wet forests) as a driver of photosynthetic activity (Restrepo-Coupe et al., 2017; Saleska et al., 2016; Wu et al., 2016). Uribe et al. (2021) found that photosynthetic activity in wet forest across the tropics is positively related to solar radiation. High cloud cover during the rainiest months reduces solar radiation. Thus, a negative correlation between rainfall and tree growth would be expected. Also, Wu et al. (2016) showed a relationship between mature leaf phenological phases with dryer months across Amazonian wet forests. Similarly, Green et al., (2020) found that vegetation greenness based on NDVI was positively correlated to the driest period in the wettest regions of the Amazon basin, interpreting their results as the combined effect of high solar radiation and high vapor pressure deficit. These two combined variables facilitate leaf transpiration and, ultimately, leaf photosynthetic activity. Then, our results are consistent with other studies about the role of light availability and likely cloudiness as limiting factors of forest productivity in ever-wet forests.

In contrast to the species discussed above, *Q. lineata* and *G. glabra* showed a positive relationship between growth rate and soil water availability. In these species, the tree-ring indices positively correlated with precipitation of the rainiest months (Figure 5). Soil water excess and low solar radiation could be limiting growth factors for some tree species in this region, but certainly not for the entire tree community, as showed in the results from this study. In some species, tree-ring formation may be genetically determined and expressed independently of

environmental seasonality (Baker, Santos, Gloor, & Brienen, 2017). Adaptations of tree growth seasonality may have arisen in distinct environments, different from the Chocó region where our study individuals occur. This idea is supported by reports of annual tree-ring in six of our tree species growing under contrasting environmental conditions: *C. racemosa, A. macropetala* and *C. elastica* have been reported in tropical seasonal forests (Brienen et al., 2009; Cintra et al., 2013; Soliz-Gamboa et al., 2011); *H. brasiliensis*, *S. globulifera*, and *G. glabra* were reported in seasonal moist or flooded forests (Callado, Da Silva Neto, Scarano, & Costa, 2001; Lotfiomran & Köhl, 2017; Ohashi, Sahri, Yoshizawa, & Itoh, 2001; Oliveira et al., 2014). Also, *G. glabra* and *Q. lineata* are widely distributed across the water availability gradient (Fig. S5). *G. glabra* is a long-lived pioneer tree with broad physiological tolerances to water and light availability (Huc, Ferhi, & Guehl, 1994; Santos, Santos, Nascimento, & Tabarelli, 2012). *Q. lineata* is a shade-tolerant species distributed through most of the Chocó region, but *Qualea* genus is broadly distributed in South American forests, from dry to wet forests (Fig. S5), indicating that the same tree species could express annual tree-rings under contrasting environments. These observations suggest that tree-ring formation could be genetically controlled overriding seasonal environmental drivers. In this way, some tree species that recently colonized ever-wet tropical forests can express tree ring due to the genetic conserved response to their original precipitation regimes. Then, tree ring formation and their response to environmental drivers should be evaluated on multiple populations of the same species to determine their environmental and genetic components.

Our study provides evidence of annual growth rhythms and tree-ring formation in ever-wet tropical forests. Previous dendrochronological studies have discovered annual rhythms in growth rings of trees and shrubs distributed around many different tropical ecosystems: from mangroves

to the limit of woody vegetation at about 5,000 m asl; from woodland savannas to dry and flooded forests (Brienen et al., 2016; Franco-Ramos, Stoffel, & Ballesteros-Cánovas, 2019; Kerr, Horn, Grissino-Mayer, & Stachowiak, 2018; Locosselli et al., 2020; Requena-Rojas, Amoroso, Ticse-Otarola, & Crispin-Delacruz, 2021; Rodriguez-Caton et al., 2021; J. Schöngart et al., 2017). Here we include new evidences of annual tree-ring in the last unexplored frontier, the ever-wet tropical forests.

We found that tree growth rates are limited in the rainiest period, in these ever-wet environments, in agreement with the expectations from Shelford's law. However, the environmental drivers affecting tree growth could be direct because of high soil moisture for root functioning (i.e., hypoxia), or indirect via light limitation caused by high cloudiness. In addition, some tree species can maintain a positive correlation with rainfall under these ever-wet conditions, suggesting the role of genetic controls and local adaptation.

Our results support the hypothesis that tree growth is reduced at the wetter-end of the precipitation range due to multiple environmental factors. These findings challenge the established paradigm of no tree-growth seasonality in the wetter-end tropical forests, which has direct implications for satellite biomass growth estimates and current global vegetation models that aim to simulate the tropical carbon sink under climatic change. The humped relationship between forest productivity (i.e., wood formation) and precipitation should be included in global vegetation models improving the CO_2 assimilation rate in the ever-wet forests (Friend et al., 2019) that represent at least 30% of the current tropical ecosystems in the world (Underwood et al., 2014).

Data availability statement

Datasets are open and freely available via Zenodo: https://doi.org/10.5281/zenodo.7521524 (Giraldo et al., 2023).

Conflict of interest

The authors declare that they have no conflict of interest.

Acknowledgements

We would like to thank the ^{14}C Analysis Facility of Max Planck Institute for Biogeochemistry for sample processing. In addition, we thank the "Tropical Dendroecology Laboratory" of the Department of Forest Sciences of the National University of Colombia and MEDEL Herbarium. We thank "Pedro Antonio Pineda Tropical Forestry Center" of the University of Tolima and those people who help us during sampling: Amalia Forero, Faber Hernández, Sixto Cáseres, Iris Valencia, Andrés Caro, and Jorge Mario Velez. We thank to Natalia Restrepo-Coupe, Daniel Zuleta and Manuel Bernal that with their comments improved the manuscript. Finally, we thank Andrés Oliveros for sharing the picture of the forest taken with a drone. Field work permits were given by National Authority for Environmental Licensing (ANLA) in the framework Permit for the Collection of Specimens of Wild Species of Biological Diversity for Non-Commercial Scientific Research Purposes granted to the National University of Colombia through Resolution 0255 of March 12, 2014, clarified by Resolution 0404 of April 30, 2014 and modified by Resolutions 1482 of November 20, 2015, 701 of July 8, 2016, 01435 of September 3, 2018, 00277 of February 18, 2020 and 01721 of October 20, 2020. Funding was provided from Minciencias Project 1118-714-51372. Max Planck Institute for Biogeochemistry, J.A. Giraldo

and S. González-Caro was supported by Minciencias in the announcement 785. T. Taylor was supported by National Science Foundation grants #1754163 and #2111028.

Author contributions

Jorge I. del Valle, Carlos A. Sierra and Jorge A. Giraldo contributed study conception and design. Sampling was conducted by Diego A. David and Jorge A. Giraldo. Data acquisition and statistical analysis were conducted by Jorge A. Giraldo, Sebastian González-Caro and Diego A. David. Jorge A. Giraldo wrote the draft of the manuscript and Jorge I. del Valle, Carlos A. Sierra, Sebastian González-Caro, Conrado Tobón, Tyeen Taylor helped to interpret data and to improve the drafts. All the authors discussed and agreed to the final version.

References

Albert, L. P., Restrepo-Coupe, N., Smith, M. N., Wu, J., Chavana-Bryant, C., Prohaska, N., … Saleska, S. R. (2019). Cryptic phenology in plants: Case studies, implications, and recommendations. *Global Change Biology*, *25*(11), 3591–3608. https://doi.org/10.1111/gcb.14759

Araza, A., de Bruin, S., Herold, M., Quegan, S., Labriere, N., Rodriguez-Veiga, P., … Lucas, R. (2022). A comprehensive framework for assessing the accuracy and uncertainty of global above-ground biomass maps. *Remote Sensing of Environment*, *272*(February). https://doi.org/10.1016/j.rse.2022.112917

Avitabile, V., Herold, M., Heuvelink, G. B. M., Lewis, S. L., Phillips, O. L., Asner, G. P., … Willcock, S. (2016). An integrated pan-tropical biomass map using multiple reference datasets. *Global Change Biology*, *22*(4), 1406–1420. https://doi.org/10.1111/gcb.13139

Babst, F., Alexander, M. R., Szejner, P., Bouriaud, O., Klesse, S., Roden, J., … Trouet, V. (2014). A tree-ring perspective on the terrestrial carbon cycle. *Oecologia*, *176*(2), 307–322. https://doi.org/10.1007/s00442-014-3031-6

Babst, F., Bodesheim, P., Charney, N., Friend, A. D., Girardin, M. P., Klesse, S., … Evans, M. E. K. (2018). When tree rings go global: Challenges and opportunities for retro- and prospective insight. *Quaternary Science Reviews*, *197*, 1–20. https://doi.org/10.1016/j.quascirev.2018.07.009

Baker, J. C. A., Santos, G. M., Gloor, M., & Brienen, R. J. W. (2017). Does Cedrela always form annual rings? Testing ring periodicity across South America using radiocarbon dating. *Trees*, *31*(6), 1999–2009. https://doi.org/10.1007/s00468-017-1604-9

Beer, C., Reichstein, M., Tomelleri, E., Ciais, P., Jung, M., Carvalhais, N., … Papale, D. (2010). Terrestrial gross carbon dioxide uptake: Global distribution and covariation with climate. *Science*, *329*(5993), 834–838. https://doi.org/10.1126/science.1184984

Borchert, R., & Rivera, G. (2001). Photoperiodic control of seasonal development and dormancy in tropical stem-succulent trees. *Tree Physiology*, *21*(4), 213–221. https://doi.org/10.1093/treephys/21.4.213

Breitsprecher, A., & Bethel, J. (1990). Stem-growth periodicity of trees in a tropical wet forest of Costa Rica. *Ecology*, *71*(3), 1156–1164.

Brienen, R., Lebrija-trejos, E., Breugel, M. Van, Perez-Garcia, E., Bongers, F., Meave, J. A., & Martínez-ramos, M. (2009). The potential of tree rings for the study of forest succession in Southern Mexico. *Biotropica*, *41*(2), 186–195. https://doi.org/10.1111/j.1744-7429.2008.00462.x

Brienen, R., Schöngart, J., & Zuidema, P. (2016). Tree rings in the tropics: Insights into the ecology and climate sensitivity of tropical trees. In G. Goldstein & S. L. Santiago (Eds.),

Tropical Tree Physiology (pp. 441–461). https://doi.org/10.1007/978-3-319-27422-5

Bunn, A. G. (2008). A dendrochronology program library in R (dplR). *Dendrochronologia*, *26*(2), 115–124. https://doi.org/10.1016/j.dendro.2008.01.002

Bunn, A. G. (2010). Statistical and visual crossdating in R using the dplR library. *Dendrochronologia*, *28*(4), 251–258. https://doi.org/10.1016/j.dendro.2009.12.001

Callado, C., Da Silva Neto, S., Scarano, F., & Costa, C. (2001). Periodicity of growth rings in some flood-prone trees of the Atlantic Rain Forest in Rio de Janeiro, Brazil. *Trees*, *15*(8), 492–497. https://doi.org/10.1007/s00468-001-0128-4

Cintra, B. B. L., Schietti, J., Emillio, T., Martins, D., Moulatlet, G., Souza, P., … Schöngart, J. (2013). Productivity of aboveground coarse wood biomass and stand age related to soil hydrology of Amazonian forests in the Purus-Madeira interfluvial area. *Biogeosciences Discussions*, *10*(4), 6417–6459. https://doi.org/10.5194/bgd-10-6417-2013

Clark, D. A., & Clark, D. B. (1994). Climate-induced annual variation in canopy tree growth in a Costa Rican Tropical Rain Forest. *Journal of Ecology*, *82*(4), 865–872.

CONIF. (1996). *Investigación Forestal del Pacífico Colombiano*. Santa fé de Bogotá.

Cook, E. R., & Kairiukstis, L. (1992). *Methods of dendrochronology: Applications in the environmental science*. Dordrecht: Kluwer Academic Publishers.

Cook, E. R., & Pederson, N. (2011). Uncertainty, Emergence, and Statistics in Dendrochronology. In M. K. Hughes, T. W. Swetnam, & H. F. Diaz (Eds.), *Dendroclimatology, Developments in Paleoenvironmental Research* (pp. 77–112). https://doi.org/10.1007/978-1-4020-5725-0_4

Corlett, R. T. (2016). The Impacts of Droughts in Tropical Forests. *Trends in Plant Science*, *21*(7), 584–593. https://doi.org/10.1016/j.tplants.2016.02.003

Costa, F. R. C., Schietti, J., Stark, S. C., & Smith, M. N. (2022). The other side of tropical forest

drought: do shallow water table regions of Amazonia act as large-scale hydrological refugia from drought? *New Phytologist*. https://doi.org/10.1111/nph.17914

De Micco, V., Carrer, M., Rathgeber, C. B. K., Julio Camarero, J., Voltas, J., Cherubini, P., & Battipaglia, G. (2019). From xylogenesis to tree rings: Wood traits to investigate tree response to environmental changes. *IAWA Journal*, *40*(2), 155–182. https://doi.org/10.1163/22941932-40190246

del Valle, J. I., & Giraldo, J. A. (2021). Radiocarbon and dendrochronology applied in a legal dispute: A case from Colombia. *Radiocarbon*, *63*(4), 1215–1223. https://doi.org/10.1017/RDC.2020.30

del Valle, J. I., Guarín, J. R., & Sierra, C. A. (2014). Unambiguous and low-cost determination of growth rates and ages of tropical trees and palms. *Radiocarbon*, *56*(1), 39–52. https://doi.org/10.2458/56.16486

Dezzeo, N., Worbes, M., Ishii, I., & Herrera, R. (2003). Annual tree rings revealed by radiocarbon dating in seasonally flooded forest of the Mapire river, a tributary of the lower Orinoco river, Venezuela. *Plant Ecology*, *168*(1), 165–175. https://doi.org/10.1023/A:1024417610776

Esquivel-Muelbert, A., Baker, T. R., Dexter, K. G., Lewis, S. L., ter Steege, H., Lopez-Gonzalez, G., … Phillips, O. L. (2017). Seasonal drought limits tree species across the Neotropics. *Ecography*, *40*(5), 618–629. https://doi.org/10.1111/ecog.01904

Esteban, E. J. L., Castilho, C. V., Melgaço, K. L., & Costa, F. R. C. (2021). The other side of droughts: wet extremes and topography as buffers of negative drought effects in an Amazonian forest. *New Phytologist*, *229*(4), 1995–2006. https://doi.org/10.1111/nph.17005

Estupinan-Suarez, L. M., Gans, F., Brenning, A., Gutierrez-Velez, V. H., Londono, M. C., Pabon-Moreno, D. E., … Mahecha, M. D. (2021). A Regional Earth System Data Lab for

Understanding Ecosystem Dynamics: An Example from Tropical South America. *Frontiers in Earth Science*, *9*(July), 1–20. https://doi.org/10.3389/feart.2021.613395

Faber-Langendoen, D., & Gentry, A. H. (1991). The structure and diversity of rain forests at Bajo Calima, Choco Region, Western Colombia. *Biotropica*, *23*(1), 2–11.

Franco-Ramos, O., Stoffel, M., & Ballesteros-Cánovas, J. A. (2019). Reconstruction of debris-flow activity in a temperate mountain forest catchment of central Mexico. *Journal of Mountain Science*, *16*(9), 2096–2109. https://doi.org/10.1007/s11629-019-5496-6

Friend, A. D., Eckes-Shephard, A. H., Fonti, P., Rademacher, T. T., Rathgeber, C. B. K., Richardson, A. D., & Turton, R. H. (2019). On the need to consider wood formation processes in global vegetation models and a suggested approach. *Annals of Forest Science*, *76*(2), 49. https://doi.org/10.1007/s13595-019-0819-x

Frumau, A., Bruijnzeel, S., & Tobón, C. (2006). *Hydrological measurement protocol for montane cloud forest. Annex 2, Final Technical Report DFID-FRP Project R7991.* Amsterdam.

Fyllas, N. M., Bentley, L. P., Shenkin, A., Asner, G. P., Atkin, O. K., Díaz, S., … Malhi, Y. (2017). Solar radiation and functional traits explain the decline of forest primary productivity along a tropical elevation gradient. *Ecology Letters*, *20*(6), 730–740. https://doi.org/10.1111/ele.12771

Gentry, A. H. (1989). Species richness and floriscti composition of choco region plant communities. *Caldasia*, *15*(71–75).

Giraldo, J. ., del Valle, J., Gonzalez-Caro, S., David, D., Taylor, T., Tobón, C., & Sierra, C. A. (2023). *Tree growth periodicity in the ever-wet tropical forest of the Americas: Datasets [Data set]*. https://doi.org/https://doi.org/10.5281/zenodo.7521524

Giraldo, J. A., del Valle, J. I., González-Caro, S., & Sierra, C. A. (2022). Intra-annual isotope

variations in tree rings reveal growth rhythms within the least rainy season of an ever-wet tropical forest. *Trees*, *36*(3), 1039–1052. https://doi.org/10.1007/s00468-022-02271-7

Giraldo, J. A., del Valle, J. I., Sierra, C. A., & Melo, O. (2020). Dendrochronological potential of trees from America's rainiest region. In M. Pompa-García & J. J. Camarero (Eds.), *Latin American Dendroecology* (pp. 79–119). https://doi.org/10.1007/978-3-030-36930-9_5

Hammond, W. M., Yu, K., Wilson, L. A., Will, R. E., Anderegg, W. R. L., & Adams, H. D. (2019). Dead or dying? Quantifying the point of no return from hydraulic failure in drought-induced tree mortality. *New Phytologist*, *223*(4), 1834–1843. https://doi.org/10.1111/nph.15922

Huc, R., Ferhi, A., & Guehl, J. M. (1994). Pioneer and late stage tropical rainforest tree species (French Guiana) growing under common conditions differ in leaf gas exchange regulation, carbon isotope discrimination and leaf water potential. *Oecologia*, *99*(3–4), 297–305. https://doi.org/10.1007/BF00627742

Karger, D. N., Conrad, O., Böhner, J., Kawohl, T., Kreft, H., Soria-Auza, R. W., … Kessler, M. (2017). Climatologies at high resolution for the earth's land surface areas. *Scientific Data*, *4*, 1–20. https://doi.org/10.1038/sdata.2017.122

Kato, S., Loeb, N. G., Rose, F. G., Doelling, D. R., Rutan, D. A., Caldwell, T. E., … Weller, R. A. (2013). Surface irradiances consistent with CERES-derived top-of-atmosphere shortwave and longwave irradiances. *Journal of Climate*, *26*(9), 2719–2740. https://doi.org/10.1175/JCLI-D-12-00436.1

Kerr, M. T., Horn, S. P., Grissino-Mayer, H. D., & Stachowiak, L. A. (2018). Annual growth zones in stems of Hypericum irazuense (Guttiferae) in the Costa Rican páramos. *Physical Geography*, *39*(1), 38–50. https://doi.org/10.1080/02723646.2017.1340714

Konings, A. G., Saatchi, S. S., Frankenberg, C., Keller, M., Leshyk, V., Anderegg, W. R. L., …

Zuidema, P. A. (2021). Detecting forest response to droughts with global observations of vegetation water content. *Global Change Biology*, *27*(23), 6005–6024. https://doi.org/10.1111/gcb.15872

Locosselli, G. M., Brienen, R. J. W., Leite, M. de S., Gloor, M., Krottenthaler, S., Oliveira, A. A. de, … Buckeridge, M. (2020). Global tree-ring analysis reveals rapid decrease in tropical tree longevity with temperature. *Proceedings of the National Academy of Sciences*, *117*(52), 33358–33364. https://doi.org/10.1073/pnas.2003873117

Lotfiomran, N., & Köhl, M. (2017). Retrospective analysis of growth A contribution to sustainable forest management in the tropics. *IAWA Journal*, *38*(3), 297–312. https://doi.org/10.1163/22941932-20170173

Lüttge, U., & Hertel, B. (2009). Diurnal and annual rhythms in trees. *Trees - Structure and Function*, *23*(4), 683–700. https://doi.org/10.1007/s00468-009-0324-1

McDowell, N., Allen, C. D., Anderson-Teixeira, K., Brando, P., Brienen, R., Chambers, J., … Xu, X. (2018). Drivers and mechanisms of tree mortality in moist tropical forests. *New Phytologist*, *219*(3), 851–869. https://doi.org/10.1111/nph.15027

McDowell, N. G., Coops, N. C., Beck, P. S. A., Chambers, J. Q., Gangodagamage, C., Hicke, J. A., … Allen, C. D. (2015). Global satellite monitoring of climate-induced vegetation disturbances. *Trends in Plant Science*, *20*(2), 114–123. https://doi.org/10.1016/j.tplants.2014.10.008

Mesa, O. J., & Rojo, J. D. (2020). On the general circulation of the atmosphere around Colombia. *Revista de La Academia Colombiana de Ciencias Exactas, Físicas y Naturales*, *44*(172), 857–875. https://doi.org/10.18257/raccefyn.899

Muller-Landau, H. C., Cushman, K. C., Arroyo, E. E., Martinez Cano, I., Anderson-Teixeira, K. J., & Backiel, B. (2021). Patterns and mechanisms of spatial variation in tropical forest

productivity, woody residence time, and biomass. *New Phytologist*, *229*, 3065–3087. https://doi.org/10.1111/nph.17084

Myers, N., Mittermeler, R. A., Mittermeler, C. G., Da Fonseca, G. A. B., & Kent, J. (2000). Biodiversity hotspots for conservation priorities. *Nature*, *403*(6772), 853–858. https://doi.org/10.1038/35002501

Ohashi, Y., Sahri, M. H., Yoshizawa, N., & Itoh, T. (2001). Annual rhythm of xylem growth in rubberwood (*Hevea brasiliensis*) trees grown in Malaysia. *Holzforschung*, *55*(2), 151–154. https://doi.org/10.1515/HF.2001.024

Oliveira, M., Mattos, P., Muñoz-Braz, E., Canetti, A., Basso, A., & Rosot, N. (2014). Growth pattern of *Qualea albiflora* and *Goupia glabra* in Amazon forest, Mato Grosso State, Brazil. *The International Forestry Review*, *16*(5), 2014. IUFRO.

Pan, Y., Birdsey, R. A., Fang, J., Houghton, R., Kauppi, P. E., Kurz, W. A., … Hayes, D. (2011). A large and persistent carbon sink in the world's forests. *Science*, *333*(6045), 988–993. https://doi.org/10.1126/science.1201609

Pearl, J. K., Keck, J. R., Tintor, W., Siekacz, L., Herrick, H. M., Meko, M. D., & Pearson, C. L. (2020). New frontiers in tree-ring research. *Holocene*, *30*(6), 923–941. https://doi.org/10.1177/0959683620902230

Pérez-Escobar, O., Lucas, E., Jaramillo, C., Monro, A., Morris, S., Borgarin, D., … Antonelli, A. (2019). The Origin and Diversification of the Hyperdiverse Flora in the Chocó Biogeographic Region. *Frontiers in Plant Science*, *10*, 1–9. https://doi.org/10.3389/fpls.2019.01328

Posada, J. M., & Schuur, E. A. G. (2011). Relationships among precipitation regime, nutrient availability, and carbon turnover in tropical rain forests. *Oecologia*, *165*(3), 783–795. https://doi.org/10.1007/s00442-010-1881-0

Poveda, G. G., & Mesa, O. J. (2000). On the existence of Lloró (the rainiest locality on Earth): enhanced ocean-land-atmosphere interaction by a low-level jet. *Geophysical Research Letters*, *27*(11), 1675–1678. https://doi.org/10.1029/1999GL006091

R Core Team, C. (2020). *R: A language and environment for statistical computing*. Retrieved from https://www.r-project.org/

Requena-Rojas, E. J., Amoroso, M. M., Ticse-Otarola, G., & Crispin-Delacruz, D. B. (2021). Assessing Dendrochronological Potential of Escallonia myrtilloides in the High Andes of Peru. *Tree-Ring Research*, *77*(2), 41–52. https://doi.org/10.3959/TRR2019-8

Restrepo-Coupe, N., da Rocha, H. R., Hutyra, L. R., da Araujo, A. C., Borma, L. S., Christoffersen, B., … Saleska, S. R. (2013). What drives the seasonality of photosynthesis across the Amazon basin? A cross-site analysis of eddy flux tower measurements from the Brasil flux network. *Agricultural and Forest Meteorology*, *182–183*, 128–144. https://doi.org/10.1016/j.agrformet.2013.04.031

Restrepo-Coupe, N., Levine, N. M., Christoffersen, B. O., Albert, L. P., Wu, J., Costa, M. H., … Saleska, S. R. (2017). Do dynamic global vegetation models capture the seasonality of carbon fluxes in the Amazon basin? A data-model intercomparison. *Global Change Biology*, *23*(1), 191–208. https://doi.org/10.1111/gcb.13442

Rodriguez-Caton, M., Andreu-Hayles, L., Morales, M. S., Daux, V., Christie, D. A., Coopman, R. E., … Villalba, R. (2021). Different climate sensitivity for radial growth, but uniform for tree-ring stable isotopes along an aridity gradient in Polylepis tarapacana, the world's highest elevation tree species. *Tree Physiology*, *41*(8), 1353–1371. https://doi.org/10.1093/treephys/tpab021

Rozendaal, D. M., & Zuidema, P. (2011). Dendroecology in the tropics: a review. *Trees*, *25*(1), 3–16. https://doi.org/10.1007/s00468-010-0480-3

Saleska, S. R., Wu, J., Guan, K., Araujo, A. C., Huete, A., Nobre, A. D., & Restrepo-Coupe, N. (2016). Dry-season greening of Amazon forests. *Nature*, *531*(7594), E4–E5. https://doi.org/10.1038/nature16457

Santos, G. G. A., Santos, B. A., Nascimento, H. E. M., & Tabarelli, M. (2012). Contrasting Demographic Structure of Short- and Long-lived Pioneer Tree Species on Amazonian Forest Edges. *Biotropica*, *44*(6), 771–778. https://doi.org/10.1111/j.1744-7429.2012.00882.x

Sauter, M. (2013). Root responses to flooding. *Current Opinion in Plant Biology*, *16*(3), 282–286. https://doi.org/10.1016/j.pbi.2013.03.013

Schindelin, J., Arganda-Carreras, I., Frise, E., Kaynig, V., Longair, M., Pietzsch, T., … Cardona, A. (2012). Fiji: An open-source platform for biological-image analysis. *Nature Methods*, *9*(7), 676–682. https://doi.org/10.1038/nmeth.2019

Schöngart, J., Bräuning, A., Barbosa, A., Lisi, C., & Oliveira, J. (2017). Dendroecological studies in the neotropics: History, status and future challenges. In M. . Amoroso, L. Daniels, P. . Baker, & J. . Camarero (Eds.), *Dendroecology. Ecological Studies (Analysis and Synthesis), vol 231* (pp. 35–73). https://doi.org/https://doi.org/10.1007/978-3-319-61669-8_3

Schöngart, Jochen, Piedade, M. T. F., Ludwigshausen, S., Horna, V., & Worbes, M. (2002). Phenology and stem-growth periodicity of tree species in Amazonian floodplain forests. *Journal of Tropical Ecology*, *18*(4), 581–597. https://doi.org/10.1017/S0266467402002389

Schurer, A. P., Ballinger, A. P., Friedman, A. R., & Hegerl, G. C. (2020). Human influence strengthens the contrast between tropical wet and dry regions. *Environmental Research Letters*, *15*(10). https://doi.org/10.1088/1748-9326/ab83ab

Schuur, E. A. G. (2003). Productivity and global climate revisited: The sensitivity of tropical forest growth to precipitation. *Ecology*, *84*(5), 1165–1170. https://doi.org/10.1890/0012-9658(2003)084[1165:PAGCRT]2.0.CO;2

Schweingruber, F. H., Börner, A., & Schulze, E. (2008). The evolution of plants stems in the earth's history. In F. H. Schweingruber, A. Börner, & E. Schulze (Eds.), *Atlas of Woody Plant Stems:Evolution, Structure, and Environmental Modifications* (pp. 3–26). Berlin, Heidelberg: Springer.

Shelford, V. (1931). Some Concepts of Bioecology. *Ecology*, *12*(3), 455–467.

Soliz-Gamboa, C., Rozendaal, D. M. A., Ceccantini, G., Angyalossy, V., van der Borg, K., & Zuidema, P. a. (2011). Evaluating the annual nature of juvenile rings in Bolivian tropical rainforest trees. *Trees*, *25*(17), 17–27. https://doi.org/10.1007/s00468-010-0468-z

Speer, J. H. (2010). Fundamentals of tree-ring research. *Fundamentals of Treering Research*, 333. https://doi.org/10.1080/00330124.2010.536466

Steinhof, A., Altenburg, M., & Machts, H. (2017). Sample preparation at the Jena ^{14}C Laboratory. *Radiocarbon*, *59*(3), 815–830. https://doi.org/10.1017/RDC.2017.50

Stine, A. R. (2019). Global Demonstration of Local Liebig's Law Behavior for Tree-Ring Reconstructions of Climate. *Paleoceanography and Paleoclimatology*, *34*(2), 203–216. https://doi.org/10.1029/2018PA003449

Tuck, S. L., Phillips, H. R. P., Hintzen, R. E., Scharlemann, J. P. W., Purvis, A., & Hudson, L. N. (2014). MODISTools - downloading and processing MODIS remotely sensed data in R. *Ecology and Evolution*, *4*(24), 4658–4668. https://doi.org/10.1002/ece3.1273

Underwood, E. C., Olson, D., Hollander, A. D., & Quinn, J. F. (2014). Ever-wet tropical forests as biodiversity refuges. *Nature Climate Change*, *4*(9), 740–741. https://doi.org/10.1038/nclimate2351

Uribe, M. R., Sierra, C. A., & Dukes, J. S. (2021). Seasonality of Tropical Photosynthesis: A Pantropical Map of Correlations With Precipitation and Radiation and Comparison to Model Outputs. *Journal of Geophysical Research: Biogeosciences*, *126*(11), 1–17.

https://doi.org/10.1029/2020JG006123

Wagner, F., Rossi, V., Stahl, C., Bonal, D., & Hérault, B. (2012). Water availability is the main climate driver of neotropical tree growth. *PLoS ONE*, *7*(4), 1–11. https://doi.org/10.1371/journal.pone.0034074

Worbes, M., & Junk, W. J. (1989). Dating tropical trees by means of 14C from bomb tests. *Ecology*, *70*(2), 503–507.

Wu, J., Albert, L. P., Lopes, A. P., Restrepo-Coupe, N., Hayek, M., Wiedemann, K. T., … Saleska, S. R. (2016). Leaf development and demography explain photosynthetic seasonality in Amazon evergreen forests. *Science*, *351*(6276), 972–976. https://doi.org/10.1126/science.aad5068

Zang, C., & Biondi, F. (2015). Treeclim: An R package for the numerical calibration of proxy-climate relationships. *Ecography*, *38*(4), 431–436. https://doi.org/10.1111/ecog.01335

Zuidema, P. A., Babst, F., Groenendijk, P., Trouet, V., Abiyu, A., Acuña-Soto, R., … Zhou, Z.-K. (2022). Tropical tree growth driven by dry-season climate variability. *Nature Geoscience*, (March). https://doi.org/10.1038/s41561-022-00911-8

Zuidema, P. A., Baker, P. J., Groenendijk, P., Schippers, P., van der Sleen, P., Vlam, M., & Sterck, F. (2013). Tropical forests and global change: Filling knowledge gaps. *Trends in Plant Science*, *18*(8), 413–419. https://doi.org/10.1016/j.tplants.2013.05.006

Zuidema, P. A., & Van der Sleen, P. (2022). Seeing the forest through the trees: how tree-level measurements can help understand forest dynamics. *New Phytologist*, *234*(5), 1544–1546. https://doi.org/10.1111/nph.18144

Figure Legends

Figure 1 Description of the study area. (a) Mean annual precipitation in South America with the *Chocó* Region (yellow-blue represents from dry to wet) enclosed in rectangle and the study site in the lower *Calima* River Basin (LCRB) in a smaller red rectangle (data from https://chelsa-

climate.org/) (Karger et al., 2017). (b) Walter and Lieth climate diagram for the site meteorological station: *Bajo Calima* from Institute of Hydrology, Meteorology, and Environmental Studies of Colombia – IDEAM (http://www.ideam.gov.co/). (c) Box and whisker plots for monthly rainfall days data from the meteorological station, (d) Box and whisker plot for monthly values of incoming short-wave solar radiation SWR (W m^{-2}) (from Clouds and the Earth's Radiant Energy System – CERES; https://ceres.larc.nasa.gov/) (Kato et al., 2013) and (e) Box and whisker plots for Normalized Difference Vegetation Index (NDVI) (Modis/Terra vegetation indices; https://lpdaac.usgs.gov/products/mod13q1v006/).

Figure 2 Wood anatomical features of tree rings in sampled tree species. (a) Hp: *Humiriastrum procerum* (Humiriaceae), (b) Ql: *Qualea lineata* (Vochysiaceae), (c) Am: *Apeiba macropetala* (Malvaceae), (d) Gg: *Goupia glabra* (Goupiaceae), (e) Ma: *Mabea sp* (Euphorbiaceae), (f) Ol: *Otoba latialata* (Myristicaceae), (g) Pu: *Pterandra ultramontana* (Malpighiaceae), (h) Ir: *Inga rubiginosa* (Fabaceae), (i) Ia: *Inga acreana* (Fabaceae), (j) Hb: *Hevea brasiliensis* (Euphorbiaceae), (k) Ce: *Castilla elastica* (Moraceae) (l) Cr: *Clarisia racemosa* (Moraceae), (m) Sg: *Symphonia globulifera* (Clusiaceae), (n) Tc *Tachigali colombiana* (Fabaceae). Arrows in the margin indicate the ring boundary. Tree rings are defined by the intra-annual variations of wood density (a, b, c, d, e, f, k, n), and both by intra-annual variation of wood density and bands of marginal parenchyma (g, h, i, j, l, m). See details on the anatomy in Giraldo et al., (2020).

Figure 3 (a) Relationship between dendrochronology date and calibrated radiocarbon date (n = 36) from 14 species: Am: *Apeiba macropetala*, Ce: *Castilla elastica*, Cr: *Clarisia racemosa*, Gg: *Goupia glabra*, Hb: *Hevea brasiliensis*, Hp: *Humiriastrum procerum*, Ia: *Inga acreana*, In: *Inga rubiginosa*, Ma: *Mabea* sp, Ol: *Otoba latialata*, Pu: *Pterandra ultramontana*, Ql: *Qualea lineata*,

Sg: *Symphonia globulifera* Tc: *Tachigali colombiana* (see Table S1, Figure S1-S2). The whiskers in dots are the standard deviation of each calibrated radiocarbon date. The dotted line is the fitted linear model. (b) The histogram represents the difference between corresponding dates (calibrated and dendrochronological dates).

Figure 4 Tree-ring chronologies generated in this study: (a) Hp: *Humiriastrum procerum*, (b) Ql: *Qualea lineata*, (c) Am: *Apeiba macropetala*, (d) Gg: *Goupia glabra*. The chronology index is represented in black. The blue area represents the number of replicate series (sample depth) for each year.

Figure 5 Bootstrapped correlations between tree-ring chronologies and environmental variables. The two rows of panels represent, respectively, the chronology correlations with precipitation and short-wave radiation (SWR) in W m^{-2}. (a) to (d) represent the chronology of each species and their correlations with precipitation. (e) to (h) represent the chronology of each species and their correlations with SWR. Species codes are Hp: *Humiriastrum procerum*, Ql: *Qualea lineata*, Am: *Apeiba macropetala* and Gg: *Goupia glabra.* Lowercase months refer to the previous year. Months in capitals refer to the concurrent year. Black dots indicate significant correlation ($p < 0.05$).

Figure 6 (a) Comparison between mean monthly growth for two species (Am: *Apeiaba macropetala,* and Gg: *Goupia glabra*) and environmental factors (Precipitation in millimeters, Soil moisture content-SMC expressed in volumetric units cm^3 cm^{-3} and Short-wave radiation-SWR in W m^{-2}). (b) cross-correlation function between tree species and the same environmental factors. The gapless annual dendrometer records become from different individuals: $n = 3$ (*A.*

macropetala) and $n = 6$ (*G. glabra*). Grey shading: represents the least rainy months which not implying water deficit. Black dots indicate significant correlation ($p < 0.05$).

Table 1 Descriptive statistics of four cross-dated tree species from the low *Calima* River Basin. *r*: mean series intercorrelation. *rbar*: running bar; EPS: expressed population signal; SNR: signal-to-noise ratio. MS: mean sensitivity. *($p < 0.05$).

	Humiriastrum procerum	*Qualea linneata*	*Apeiba macropetala*	*Goupia glabra*
Timespan (years)	1943-2016	1960-2016	1984-2016	1938-2019
Sampled trees (series)	6	7	5	12
Diameter range (cm)	15 - 50	10 – 60	45 - 50	10 - 30
Ring width and deviation (mm)	2.4 ±1.3	3.7 ± 2.1	8.3 ± 6.1	1.8 ± 1.1
Interseries correlation (*r*)	0.49*	0.46*	0.41*	0.42*
rbar	0.28	0.36	0.31	0.32
EPS	0.82	0.87	0.83	0.89

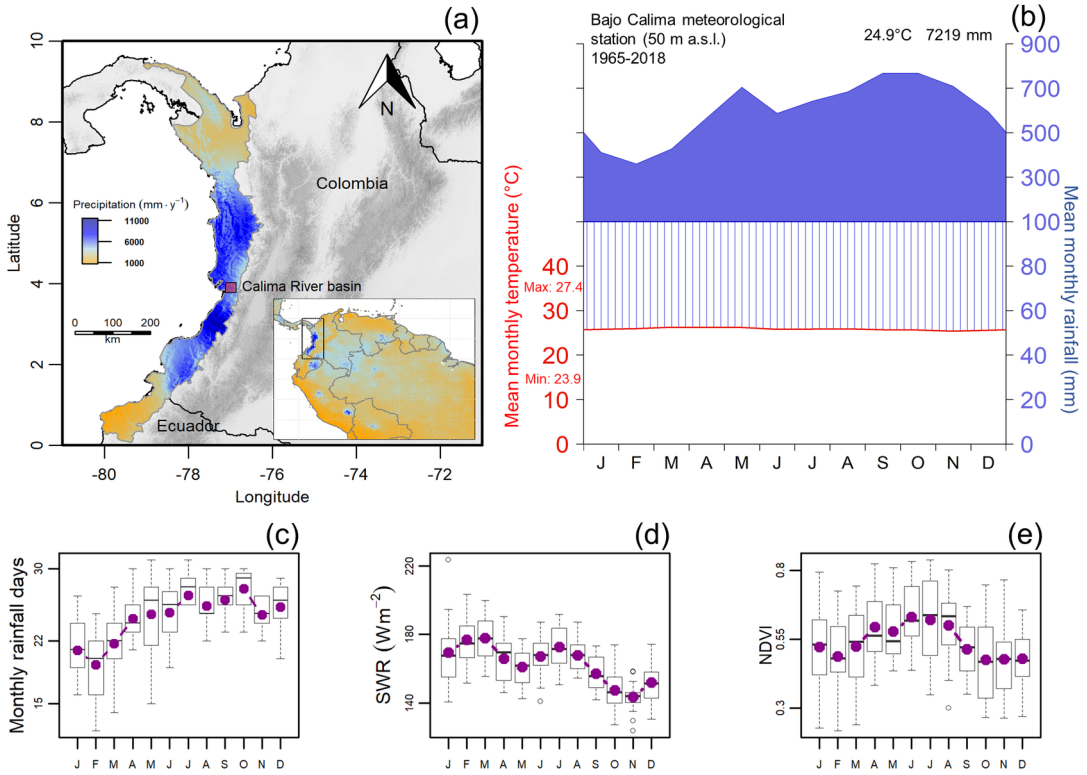

JEC_14069_Fig1.tif

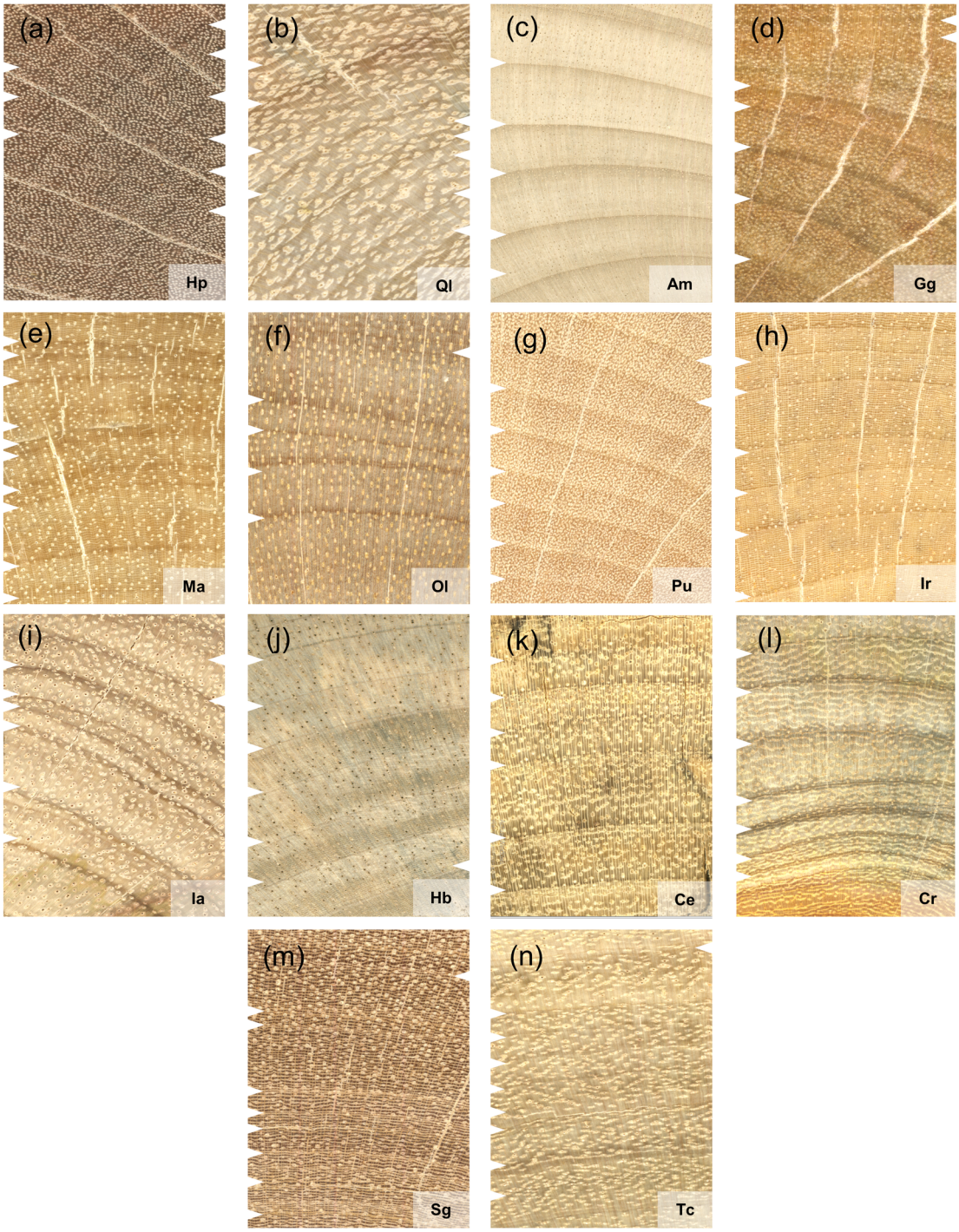

JEC_14069_Fig2.tif

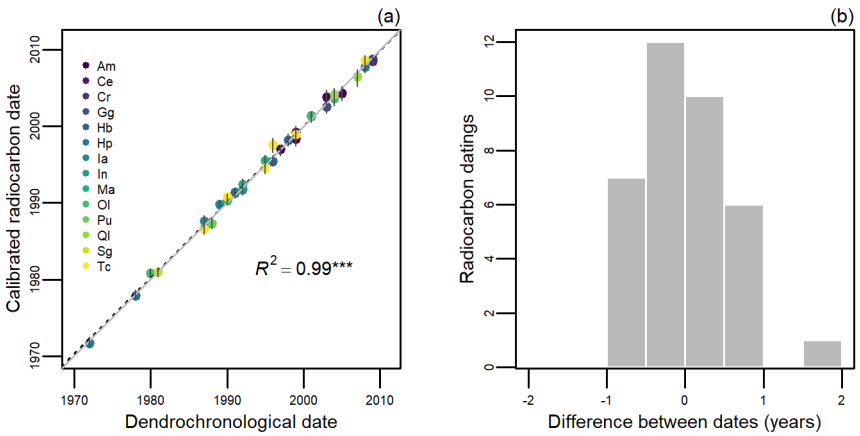

JEC_14069_Fig3.tif

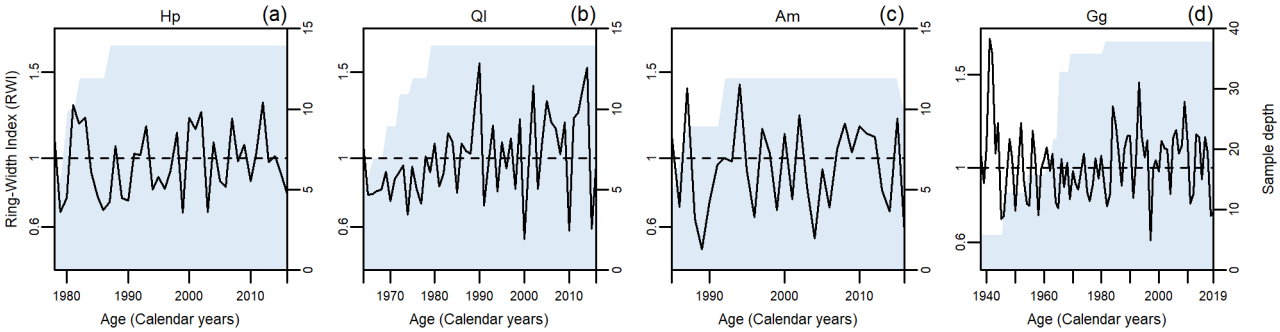

JEC_14069_Fig4.tif

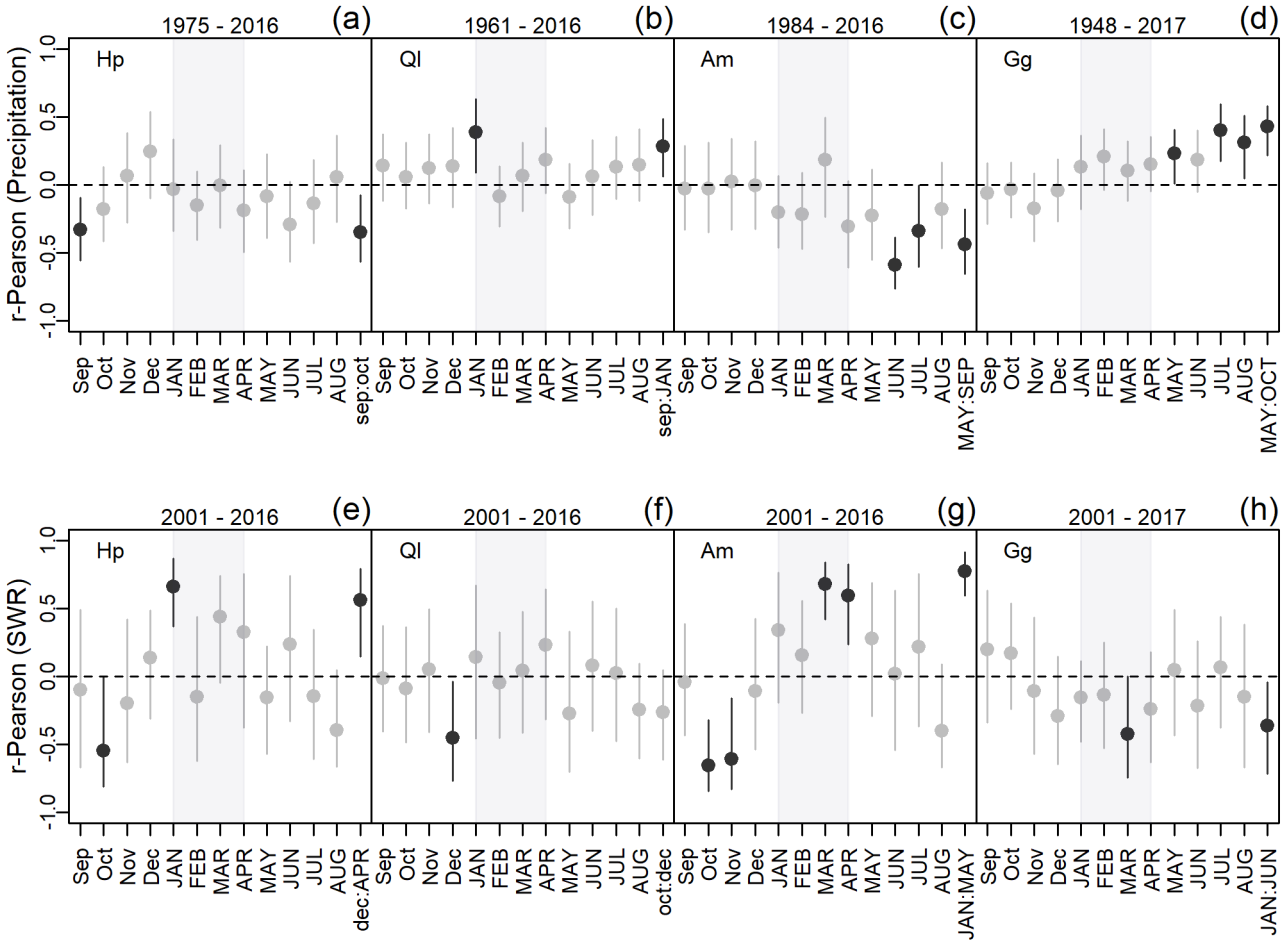

JEC_14069_Fig5.tif

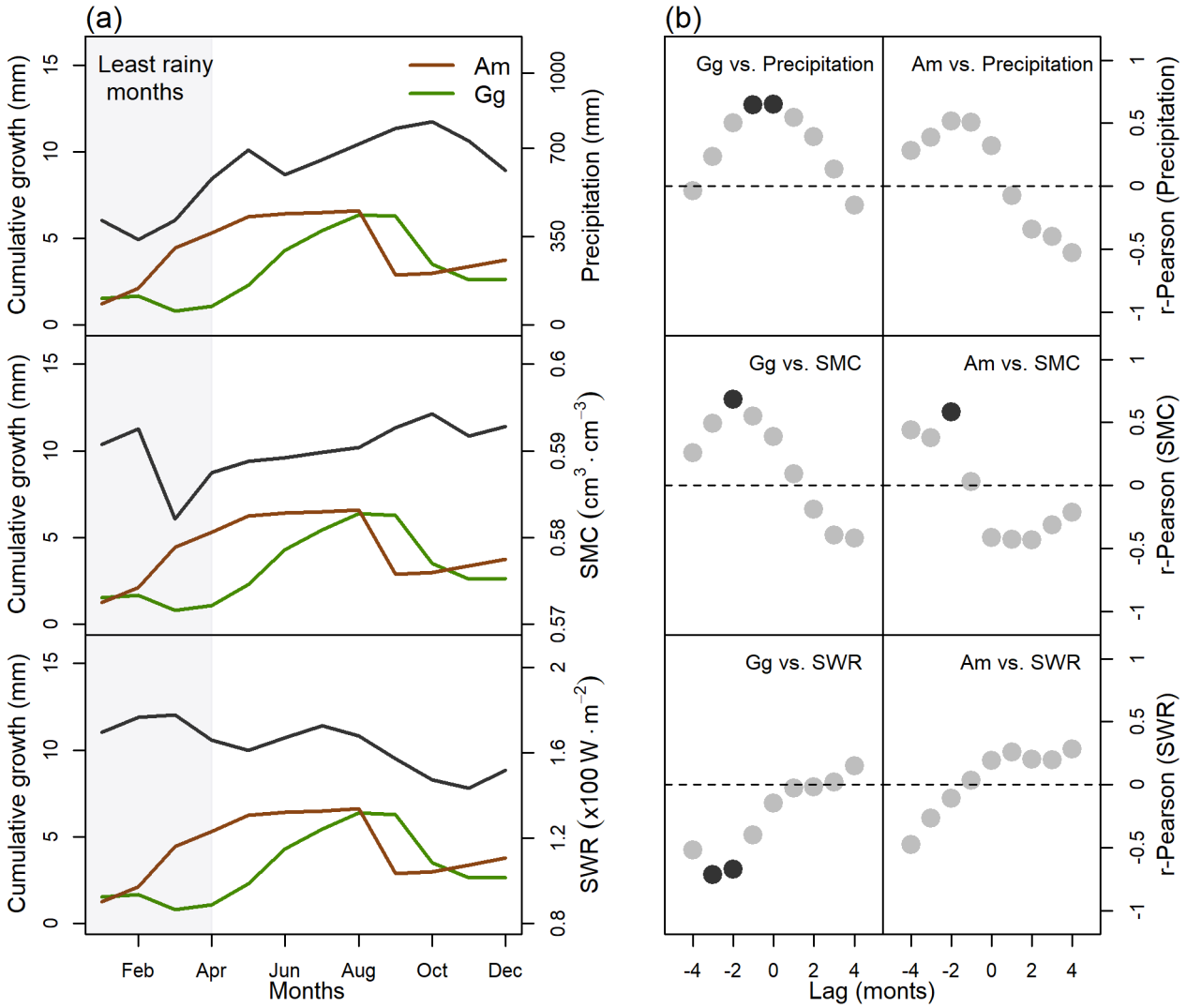

JEC_14069_Fig 6v1.tif

Table 1 Descriptive statistics of four cross-dated tree species from the low *Calima* River Basin. *r*: mean series intercorrelation. *rbar*: running bar; EPS: expressed population signal; SNR: signal-to-noise ratio. MS: mean sensitivity. *($p < 0.05$).

	Humiriastrum procerum	*Qualea linneata*	*Apeiba macropetala*	*Goupia glabra*
Timespan (years)	1943-2016	1960-2016	1984-2016	1938-2019
Sampled trees (series)	6	7	5	12
Diameter range (cm)	15 - 50	10 – 60	45 - 50	10 - 30
Ring width and deviation (mm)	2.4 ±1.3	3.7 ± 2.1	8.3 ± 6.1	1.8 ± 1.1
Interseries correlation (*r*)	0.49*	0.46*	0.41*	0.42*
rbar	0.28	0.36	0.31	0.32
EPS	0.82	0.87	0.83	0.89